ChemPubSoc Europe

DOI: 10.1002/chem.201403832

CHEMISTRY
A European Journal
Full Paper

Expanded Porphyrins

Naphthobipyrrole-Derived Sapphyrins: Rational Synthesis, Characterization, Nonlinear Optical Properties, and Excited-State Dynamics

Tridib Sarma,[a] Puliparambil Thilakan Anusha,[b] Ashok Pabbathi,[a] Soma Venugopal Rao,[b] and Pradeepta K. Panda*[a]

Abstract: Two new free-base β-octa and hexaalkyl naphthobipyrrole-derived sapphyrins are reported along with various salts thereof. One of them has substituents at all of its β positions, whereas the pyrrole unit opposite to the bipyrrolic moiety is unsubstituted in the other. The effect of bipyrrole fusion on the structure of sapphyrins was explored. Interestingly, an unprecedented sandwiched supramolecular aqua-bridged free-base sapphyrin dimer was also characterized in the solid state. Further, the effect of anions on the third-order nonlinear optical properties of these sapphyrins were explored in the salt form, along with their detailed excited-state dynamics by both degenerate and nondegenerate pump–probe studies.

Introduction

Sapphyrins belong to the class of expanded porphyrins that can be structurally derived through replacement of one of the pyrrolic moieties with a bipyrrolic unit. The resulting macrocycle, owing to its expanded core, displays affinity towards anions in its diprotonated state.[1a] Initial efforts in this area were mostly related to development of efficient synthetic routes and anion-binding abilities of these macrocycles.[1b,c] As the area of expanded porphyrins evolved tremendously in the last two decades, concomitantly sapphyrins were also explored for their potential applications as functional materials, receptors for neutral molecules for drug delivery, and as photosensitizers in photodynamic therapy.[2]

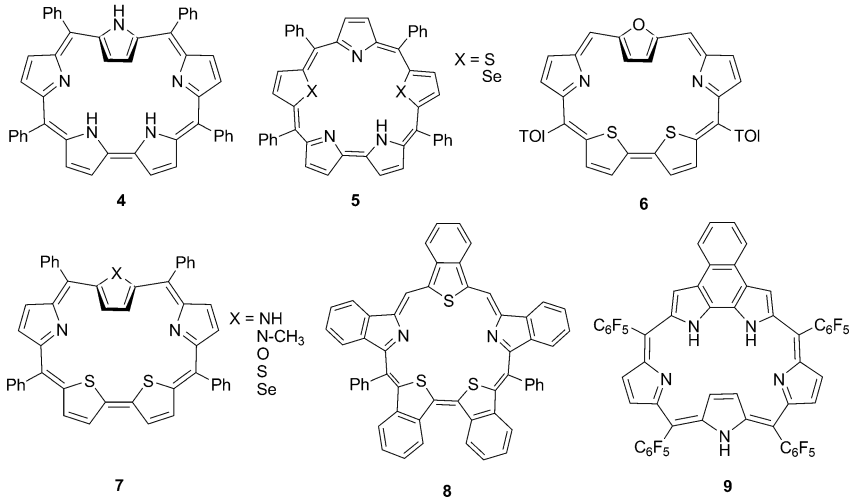

Figure 1. Structural diversity in sapphyrins.

Initial efforts in sapphyrin chemistry involved the development of efficient syntheses of decaalkyl sapphyrins. Subsequently, a large number of functionalized sapphyrins were synthesized, which include C, O, S, and Se apart from N as sapphyrin core atoms,[3] along with N-confused sapphyrins and, more recently, N-fused sapphyrins.[4]

Further, *meso*-tetraphenyl sapphyrin (**4**; Figure 1) displays interesting structural diversity, wherein the pyrrole ring opposite to the bipyrrolic entity adopts an inverted disposition with its NH group residing at the periphery away from the core. This in

[a] *Dr. T. Sarma, A. Pabbathi, Dr. P. K. Panda*
School of Chemistry
University of Hyderabad
Hyderabad-500046, Andhra Pradesh (India)
Fax: (+91)-40-2301-2460
E-mail: pkpsc@uohyd.ernet.in
pradeepta.panda@gmail.com

[b] *P. T. Anusha, Dr. S. Venugopal Rao*
Advanced Centre of Research in High Energy Materials (ACRHEM)
University of Hyderabad
Hyderabad-500046, Andhra Pradesh (India)

Supporting information for this article is available on the WWW under http://dx.doi.org/10.1002/chem.201403832.

© 2014 Wiley-VCH Verlag GmbH & Co. KGaA, Weinheim

turn undergoes a ring flip of the same pyrrole unit, producing an all-N-in conformation on protonation.[5] Subsequently, several sapphyrin derivatives were synthesized having substituents at the *meso* or β positions or both, along with core modification to study their structural diversity, in particular flipping of the pyrrole unit.[3b] ^{1}H NMR and X-ray structure analyses show that inverted structures are generally observed for larger core sizes and the presence of smaller heteroatoms (N or O) in the two flanking heterocyclic rings of the constituent tripyrromethane unit.[6] For example, Chandrashekar and co-workers reported that the presence of heavy atoms such as S or Se in these two rings leads to planar structures, as observed for **5** (Figure 1), despite its having four *meso* substituents.[7] Crystal structure analysis of these compounds by Chandrashekar and co-workers revealed the presence of NH···S and NH···Se hydrogen-bonding interactions in the macrocyclic cavity, which probably stabilize the planar structure.[7b] Further, Lee and co-workers demonstrated that ring inversion can also be effected by imposing large ring strain (in **6** and **7**) by increasing the C_α–$C_{\alpha'}$ distance of the bipyrrole moiety by replacing it with bithiophene, rather than the presence of *meso*-aryl substituents.[8] However, trithiapentabenzo sapphyrin **8** reported by Okujima et al. did not show any ring inversion owing to the presence of β substituents, despite having a similar core to **6**.[9]

Similarly, π extension could be effected by fusing various aromatic groups at the macrocyclic periphery, which thereby enhanced their absorbance in the red region. In this direction, bipyrrole fusion[10a] led to more dramatic consequences for the photophysical properties in comparison to fusion of pyrrole β positions.[10b] Latos-Grażyński and co-workers, through elaborate NMR experiments and absorption studies demonstrated the existence of an all-N-in and a pyrrole-inverted (N-out) conformer in diprotonated *meso*-tetraphenyl sapphyrin, depending on solvent polarity.[11a] On the other hand, recently we found that naphthosapphyrin **9**, synthesized by mixed condensation, in which the bipyrrolic moiety of *meso*-tetrakis(pentafluorophenyl) sapphyrin is fused with an *o*-phenylene moiety, displays very interesting re-inversion of the pyrrole ring (latter structure, i.e., inverted dicationic sapphyrin reported by Latos-Grażyński and co-workers[11a]) on addition of an excess of trifluoroacetic acid (TFA) to give a single inverted diprotonated species.[12] In any case, to obtain an inverted structure, the pyrrole ring opposite to the bipyrrole unit must be unsubstituted.[11b] However, except for *meso*-tetraaryl sapphyrins, there is no report on an unsubstituted pyrrole ring opposite to the bipyrrole moiety. In view of these developments, herein we report the synthesis of two new naphthobipyrrole-derived sapphyrins by following the rational 3+2 approach. Whereas one sapphyrin has all of its β positions substituted, the other has an unsubstituted pyrrole unit opposite to the naphthobipyrrole moiety. The idea was to see whether pyrrole flipping occurs in the latter owing to bipyrrole fusion. Further, we also evaluated their third-order nonlinear optical (NLO) properties, using the *Z*-scan technique[13] with approximately 2 ps pulses, and the effect of anions in their corresponding diprotonated salts. This was necessitated by the emergence of expanded porphyrins as a new class of attractive compounds for two-photon absorption (2PA) materials.[14–15] The 2PA coefficients and cross sections were estimated from the open-aperture *Z*-scan data, and the nonlinear refractive indices n_2 from the closed-aperture data.[16–23] We also present extensive time-resolved studies on these sapphyrins and their various salts using degenerate and nondegenerate picosecond pump–probe measurements to study their excited-state dynamics. A systematic study on the NLO properties and excited-state dynamics of sapphyrins with different counteranions has not been reported so far.

Results and Discussion

Synthesis of naphthosapphyrins

The new naphthosapphyrins were synthesized by following a rational MacDonald-type 3+2 approach in which β-dialkylated naphthobipyrrole dialdehyde **2** (employed to increase the solubility of the resultant macrocycles)[24] was condensed with tripyrrane diacid **3a** or **3b** in acidified (*p*-TsOH) ethanol in the presence of oxygen to form the desired naphthosapphyrins **1a** and **1b** in 18 and 26% yield, respectively (Scheme 1). Compound **3b**, previously unknown, was synthesized by following the synthetic route of **3a**.[10a,25] The sapphyrins were characterized by NMR and UV/Vis spectroscopy and HRMS. Further, sapphyrin **1a** was characterized in the diprotonated (chloride) and monoprotonated (acetate) states, whereas sapphyrin **1b** was characterized in the free-base form, by single-crystal X-ray diffraction. *meso*-Tetraaryl naphthosapphyrin **9** was reported recently by Lee et al. in collaboration with Sessler, Kim and us,[12] whereby **9** was synthesized by a 2+1+1+1 strategy in the presence of TFA in very low yield (ca. 2%) along with the dinaphthorosarin.

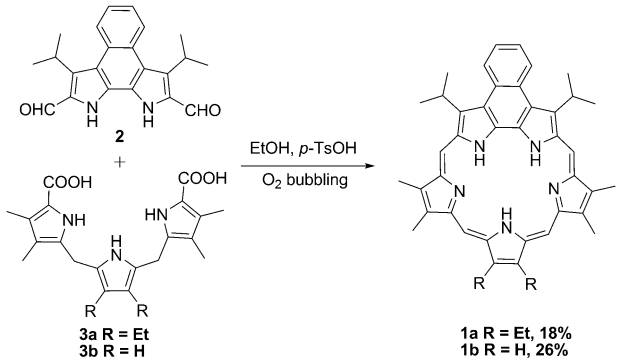

Scheme 1. Synthesis of naphthosapphyrins **1a**,**b**.

^{1}H NMR analysis of naphthosapphyrins

The ^{1}H NMR spectrum of **1a** in $CDCl_3$ at room temperature shows a very broad NH signal at −0.51 ppm (confirmed by D_2O exchange) and signals corresponding to *meso* protons at 11.27 and 10.92 ppm. This confirms a planar structure (all-N-in), as observed for decaalkyl sapphyrins, which was expected

© 2014 Wiley-VCH Verlag GmbH & Co. KGaA, Weinheim

owing to alkyl substitution at all pyrrolic β positions.[26] In comparison to the benzosapphyrin of Lee et al.,[10a] for which three sets of NH signals were observed in the free-base form, tautomerization of NH protons seems to be more rapid in **1a**. On protonation, three sets of NH signals in 2:1:2 ratio appeared. The positions of the NH signals depends on the presence of different counteranions, as revealed by the ^{1}H NMR spectra of diprotonated **1a**, prepared by washing the free base with different protic acids (Table 1). The ^{1}H NMR spectrum of free-base

Table 1. NH and *meso*-CH chemical shifts [ppm] in ^{1}H NMR spectra of **1a** and **1b** with different counteranions in $CDCl_3$.

Compound	*meso*-CH	β-pyrrole CH	NH
1a·2HCl	11.85 (s), 11.54 (s)	–	−3.17, −3.65, −4.34
1a·H_2SO_4	11.85 (br s), 11.54 (br s)	–	−3.16, −3.71, −4.34
1a·2*p*-TsOH	11.75 (s), 11.36 (s)	–	−4.05, −4.26, −4.87
1a·2$HClO_4$	11.94 (s), 11.63 (s)	–	−5.14, −5.51, −6.41
1b·2HCl	11.96 (s), 11.65 (s)	10.35	−3.54, −3.56, −4.81
1b·2*p*-TsOH	11.85 (s), 11.47 (s)	10.31	−4.19, −4.43, −5.26
1b·2TFA	11.99 (s), 11.65 (s)	10.43	−3.91, −3.99, −5.13

1b in $CDCl_3$ shows similar trends to that of **1a**. For example, a broad signal at −0.95 ppm corresponding to NH (confirmed by D_2O exchange) confirmed the absence of any inverted conformation in the macrocycle, at least at room temperature. ^{1}H NMR spectra of diprotonated forms of **1b** show a similar pattern to that of **1a**, but relatively broad NH signals were observed. Table 1 lists the positions of the NH and *meso* signals for different counteranions. The *meso*-CH signals are not much affected by the counteranions, but significant shifts were observed for NH signals, probably owing to the different coordination modes of various counteranions with pyrrolic NH groups and the resultant strength of the hydrogen bonds. In the free-base sapphyrins **1a** and **1b**, chemical shifts and integrations of NH signals were found to depend on the amount of residual water present in the NMR solvent (Supporting Information). Since **1b** has one unsubstituted pyrrole unit opposite to the naphthobipyrrole unit, we were interested whether any inversion occurs in the presence of excess anions, as noticed in tetraaryl sapphyrins. To this end, we titrated a $CDCl_3$ solution of free-base **1b** with TFA (Figure 2). The results ruled out any kind of inversion, even in the presence of an excess of TFA, as no significant change in the spectra could be detected that could be attributed to the corresponding inverted structure.

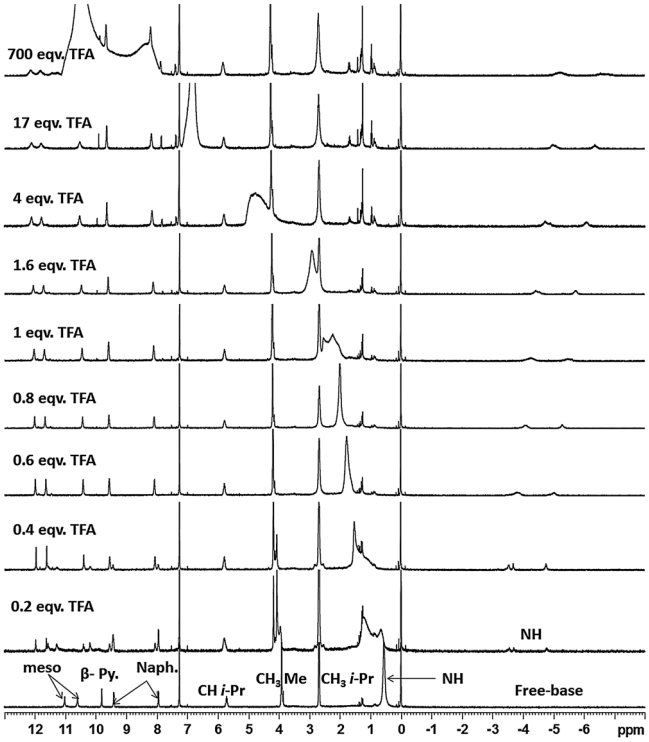

Figure 2. ^{1}H NMR titration of free-base **1b** with TFA in $CDCl_3$.

Structural analysis of naphthosapphyrins

Solid-state structures of **1a**·2HCl, **1a**·CH_3COOH (crystals obtained by slow evaporation of chloroform/hexane), and free-base **1b** (from chloroform/methanol) were determined by XRD.[27] The structure of **1a**·2HCl has a nearly planar geometry. The two N atoms of the bipyrrolic fragment (N1, N5) deviate from the mean plane defined by the sapphyrin core (excluding alkyl substituents) by 0.27 and 0.33 Å respectively. These deviations are larger than those in the benzosapphyrin (0.19 and 0.09 Å) and can be attributed to the relatively bulky nature of the naphthobipyrrole moiety compared to the benzo-fused bipyrrole unit of the latter.[10a] The other three N atoms of the tripyrrane fragment lie closer to the mean plane with deviations in the range of 0.05–0.13 Å (Figure 3). Two chloride ions were found above and below the macrocyclic core, each of which is hydrogen-bonded to three pyrrolic NH groups of the macrocycle with N···Cl distances ranging from 3.08 to 3.26 Å. The distances of these two Cl^- ions from the mean plane are 1.73 and 1.97 Å. The unsymmetrical disposition of the two chloride ions is more pronounced than that observed in analogous dichlor-

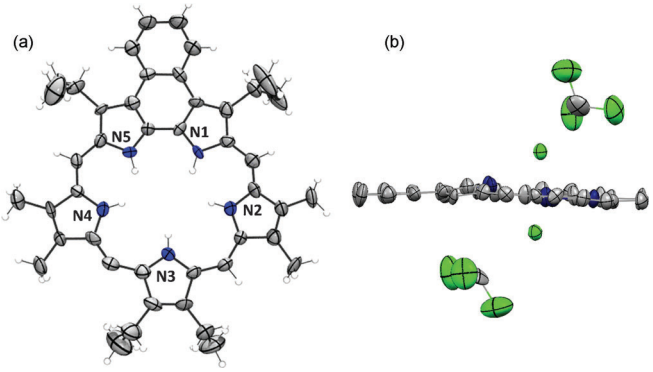

Figure 3. ORTEP of **1a·2HCl**. a) Front view. Two solvent ($CHCl_3$) molecules and chloride counteranions are omitted for clarity. b) Side view. H atoms and peripheral alkyl groups are omitted for clarity. Thermal ellipsoids are scaled to 35% probability.

© 2014 Wiley-VCH Verlag GmbH & Co. KGaA, Weinheim

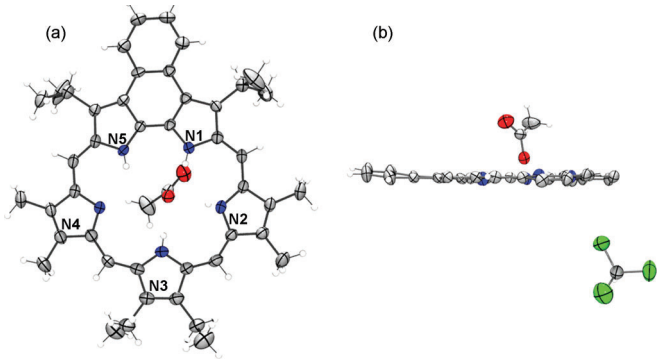

Figure 4. ORTEP of **1a**·CH_3COOH. a) Front view. One solvent ($CHCl_3$) molecule omitted for clarity. b) Side view. Peripheral alkyl groups are omitted for clarity. Thermal ellipsoids are scaled to 35% probability.

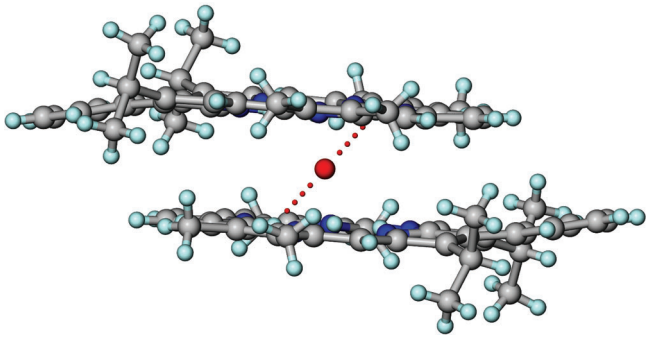

Figure 5. Supramolecular dimer of free-base naphthosapphyrin **1b**. One solvent ($CHCl_3$) molecule is omitted for clarity.

ide salts of decaalkyl (1.77 and 1.89 Å)[1a] and diphenyl sapphyrins (1.82 and 1.85 Å).[28] The N2···N4 distance is 5.54 Å. Similar N···N distances were also observed for the monoprotonated salt **1a**·CH_3COOH (Figure 4) and free-base **1b** (5.57 and 5.60 Å respectively). This value is slightly greater than that of the fluoride complex of a decaalkyl sapphyrin[29] (5.40 Å) and dihydrochloride salt of *meso*-diphenyl sapphyrin,[28] which is known to be inverted in its free-base form (5.33 Å). Sapphyrins containing bithiophene units are known to have larger core sizes, with values generally in the range of 6.23–6.39 Å,[8] and exist in inverted conformation. In comparison to **1a**·2HCl, free-base **1b** (Supporting Information) and **1a**·CH_3COOH were found to be more planar. Deviation of the N atoms of the bipyrrolic unit from the mean plane were found to be 0.075 and 0.029 Å for **1b** and 0.04 and 0.05 Å for **1a**·CH_3COOH. Likewise, N atoms of tripyrrane fragment lie closer to the mean plane with a deviation in the range from 0.04 to 0.09 Å for **1a**·CH_3COOH and 0.03 to 0.06 Å for **1b**. The solid-state structure of monoprotonated **1a**·CH_3COOH[30] (also confirmed by the UV/Vis spectrum of a solution of the crystals) reveals that the acetate ion is bound to the sapphyrin molecule through three hydrogen bonds with one of the O atoms of the acetate ion pointing towards the macrocyclic cavity at N···O distances ranging from 2.70 to 2.74 Å. Further, the acetate ion was found to reside much closer to the mean plane (1.04 Å) of the sapphyrin compared to the benzoate ion in the monobenzoate salt of decaalkyl sapphyrin derivatives (1.285 Å), which reflects the stronger interaction between the more basic acetate ion and the monoprotonated sapphyrin moiety.[31] Assuming similar core sizes of **1a** and **1b**, we can conclude that bipyrrole fusion leads to core expansion in sapphyrins, which however is not large enough to effect inversion of pyrrole moiety opposite to the bipyrrole moiety.

The crystal structure of free-base **1b** (Figure 5) shows that this compound exists in the solid state as an aqua-bridged supramolecular dimer, in which each sapphyrin unit is coordinated to a water O atom through hydrogen-bonding interaction with the N3 and N4 atoms of the tripyrrane moiety with N···O distances ranging from 2.78 to 2.99 Å. This is reflected in the strong water dependence of the NH chemical shift in the ^1H NMR spectrum of free-base **1b** (Supporting Information). To the best of our knowledge, the crystal structure of free-base sapphyrin has so far not been reported in the literature. Further, π–π stacking between the two monomeric sapphyrin units is quite strong with an interplanar distance of about 3.48 Å and centroid–centroid distance of about 3.64 Å. This type of aqua-bridged dimeric structure is unprecedented for sapphyrins in the solid state, and the only report, by Sessler et al., involves a self-assembled sapphyrin dimer in the diprotonated state, in which the interplanar distance of about 3.76 Å and centroid–centroid distance of about 7.65 Å indicate much weaker π–π stacking between the two diprotonated sapphyrin units.[32]

Ground-state absorption and emission properties of naphthosapphyrins

The absorption spectrum of free-base **1a** shows a split Soret-like band with absorption maxima at 488 nm and a shoulder at 468 nm, whereas Q-like transitions appeared at 671, 692, 730, and 765 nm (Figure 6). Thus, the Soret band and lowest-energy Q-band are redshifted by 22 and 37 nm, respectively, in comparison to benzosapphyrin.[10] Similar split Soret bands at 502 and 527 nm were also observed for the *meso*-tetraaryl analogue **9**.[12] Diprotonated **1a** displays a blueshifted Soret band (10 to 15 nm) compared to the free base. On protonation, Q bands also undergo blueshifts with a relatively intense Q-like transition in the range of 696–699 nm accompanied by a broad shoulder around 724–727 nm. The absorption patterns observed for different salts are more or less similar. All salts and the free base emit around 730 nm (Figure 6). However, the quantum yield of the free base is lower than those of its diprotonated counterparts (Table 2). The absorption spectrum of free-base **1b** shows a well-defined split Soret band at 465 and 486 nm. The Q-type absorption bands at 670, 690, 733, and 771 nm showed a similar pattern to those of **1a** (Figure 6). Diprotonated forms of **1b**, obtained by washing with aqueous solutions of different acids, show an increase in intensity of the Soret band with a marginal blueshift, accompanied by increased intensity and blueshift of the Q bands compared to the free base. Two well-resolved Q bands appeared around 699 (intense) and 731 nm. One notable difference between the two protonated naphthosapphyrins is that the splitting of the

© 2014 Wiley-VCH Verlag GmbH & Co. KGaA, Weinheim

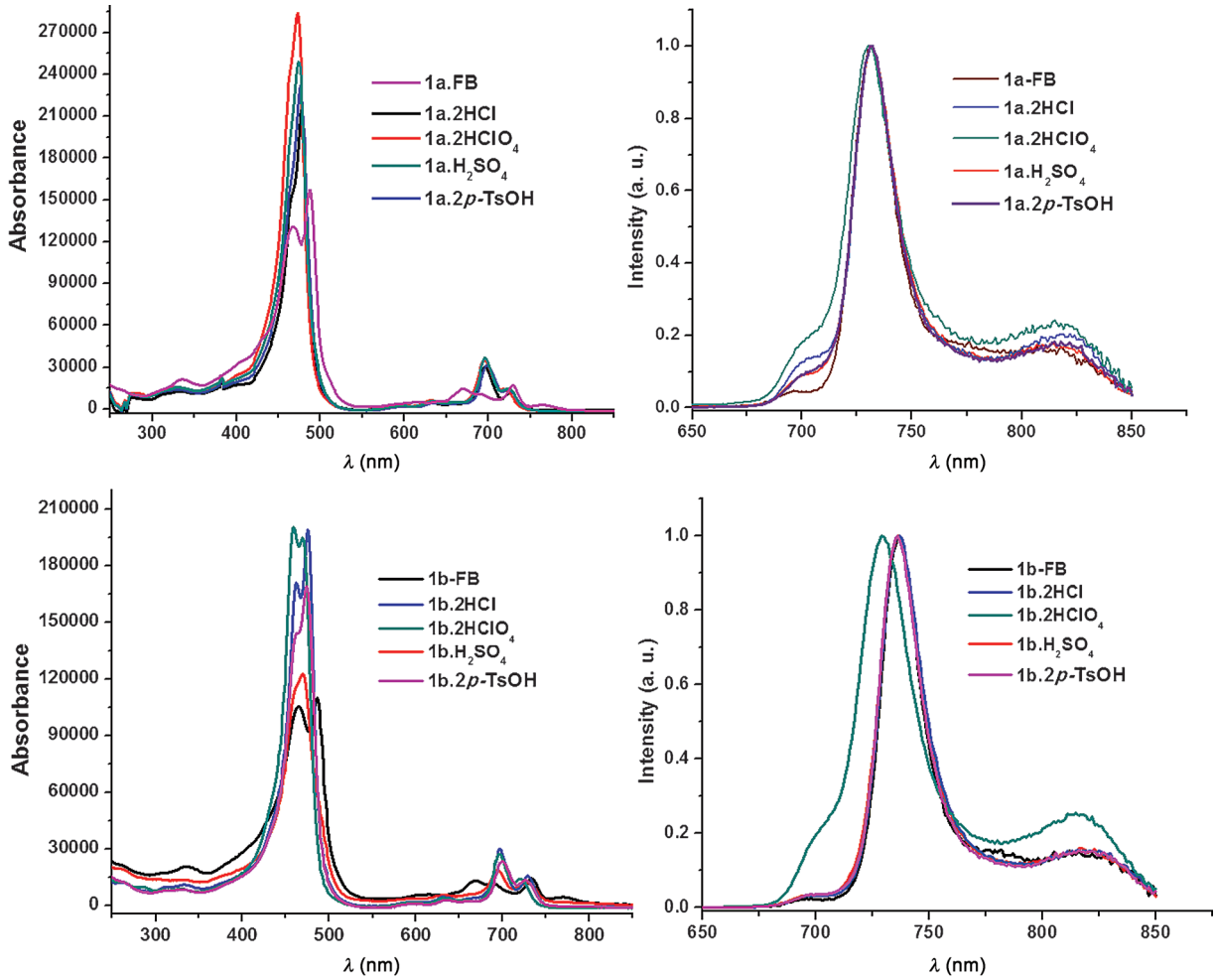

Figure 6. Top: UV/Vis (left) and normalized emission (right) spectra of naphthosapphyrin **1 a** and its diprotonated salts in $CHCl_3$. Bottom: UV/Vis (left) and normalized emission (right) spectra of naphthosapphyrin **1 b** and its diprotonated salts in $CHCl_3$.

Table 2. Absorption and emission properties of **1 a** and **1 b** in $CHCl_3$.

Compound	Solvent	Absorption		Emission		
		λ_{max} [nm]	ε [$M^{-1}cm^{-1}$]	λ_{exc} [nm]	λ_{max} [nm]	φ_f[a] [%]
1 a	$CHCl_3$	488	156000	502	732	1.3
1 a·2 HCl	$CHCl_3$	478	216000	440	731	3.8
1 a·2 $HClO_4$	$CHCl_3$	473	283000	498	730	2.1
1 a·H_2SO_4	$CHCl_3$	474	249000	497	731	5.3
1 a·2 *p*-TsOH	$CHCl_3$	476	231000	497	731	4.5
1 b	$CHCl_3$	486	109000	500	737	1.4
1 b·2 HCl	$CHCl_3$	475	199000	498	737	5.4
1 b·2 $HClO_4$	$CHCl_3$	459	200000	440	729	8.1
1 b·H_2SO_4	$CHCl_3$	470	122000	497	736	5.9
1 b·2 *p*-TsOH	$CHCl_3$	474	169000	500	736	4.3

[a] Fluorescence quantum yields were measured with tetraphenylporphyrin as reference.[33]

Soret band observed for the free base is still retained in protonated **1 b**, which was not observed in case of protonated **1 a**. Although not a confirmation, this indicates that the energy states associated with the Soret band probably do not become degenerate on protonation of **1 b** owing to large difference in the energies of the constituent pyrrolic units (alkylated versus non-alkylated pyrroles). Emission spectra of free-base **1 b** and its different salts display maxima around 736 nm, except for **1 b**·2 $HClO_4$, the emission of which is slightly blueshifted (8 nm) compared to that of **1 b** (Figure 6). To determine whether any structural change occurs in the presence of excess acid, the absorption spectrum of **1 b** was monitored during titration against TFA (Supporting Information). However, no significant change was observed, and thus any structural change, even in the presence of excess acid, is excluded (as noted in the ^1H NMR study). The fact that the spectra became almost saturated before addition of two equivalents of acid, unlike the tetraaryl analogue **9**,[12] indicated that there is not much structural difference between mono- and di-

© 2014 Wiley-VCH Verlag GmbH & Co. KGaA, Weinheim

cationic forms and that the pK_{a1} and pK_{a2} values are very similar.

Third-order NLO studies on naphthosapphyrins

Figure 7 shows the open-aperture *Z*-scan data recorded at 800 nm for all of the investigated sapphyrins. Clearly, two-photon absorption (2PA) is the dominant mechanism (also confirmed by intensity-dependent studies). Input peak intensities of $I_{00} \approx 100\ GW\,cm^{-2}$ for free bases and $I_{00} \approx 130\ GW\,cm^{-2}$ for the salt solutions were used. The occurrence of 2PA could be due to the available two-photon resonant states in the vicinity of the B bands, that is, in 400–505 nm (19800–25000 cm^{-1}) range. Interestingly, at the same peak intensity at which the free bases exhibited 2PA ($\approx 100\ GW\,cm^{-2}$), the salts did not display any nonlinearity, and only at slightly higher peak intensities ($\approx 130\ GW\,cm^{-2}$) did the salts start to exhibit nonlinear absorption behavior. Table 3 summarizes all of the NLO coefficients retrieved from the *Z*-scan data. The 2PA coefficients and cross sections (200–1100 GM) obtained for the naphthosapphyrin derivatives are slightly lower than the σ_2 values of the dihydrochloride salts of decaalkyl sapphyrins reported by Yoon et al.[34] Interestingly, the perchlorate salts showed the largest σ_2 values for both of the sapphyrin derivatives compared to their free bases and other salts. Figure 8 shows the closed-aperture *Z*-scan data of all investigated compounds. All of them exhibited negative nonlinearity of n_2, as is evident from the peak/valley structures. The values of n_2 retrieved from the fits were about $10^{-16}\ cm^2\,W^{-1}$. We could not decouple the solvent contribution in the closed-aperture mode. As the n_2 value of chloroform is positive, the n_2 values of these compounds will be higher than those presented here. The solvent contribution in the open-aperture data recorded at corresponding peak intensities is negligible.

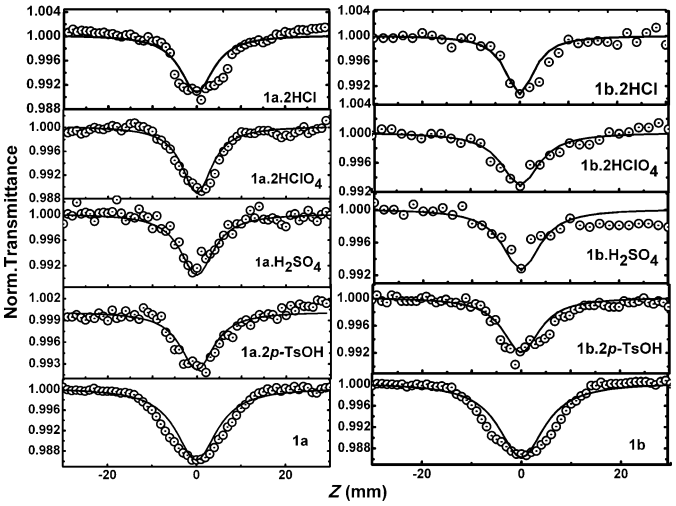

Figure 7. Open-aperture *Z*-scan data at 800 nm. The input peak intensity was approximately 100 $GW\,cm^{-2}$ for free bases and approximately 130 $GW\,cm^{-2}$ for the salt solutions. Open circles: experimental data; solid lines: 2PA fits.

Degenerate pump–probe measurements

Complete details of degenerate pump–probe experiments were presented in some of our earlier works.[19,36] The initial degenerate pump–probe measurements were performed with lower peak intensities ($\approx 100\ GW\,cm^{-2}$) of the pump beam. The initial peak intensities were such that nonlinear effects were avoided. It was observed that differential probe transmittance gave an autocorrelation-type signal. In the case of free-base samples, the pump–probe signal showed a positive rise with double-exponential decay. We believe that in this case the intensity was sufficient to excite the two-photon resonant states (supported by *Z*-scan open-aperture measurements) and the decay comprised two components. To excite the two-photon resonant states of other compounds (i.e., the sapphyrin salts), the experiments were performed at slightly higher peak intensities of the pump beam. Figure 9 shows the data for **1a**·2HCl, **1a**·2$HClO_4$, **1a**·2*p*-TsOH, **1b**·2*p*-TsOH, as well as for **1a** and **1b**, both at low and at high peak intensities. The differential probe transmittance was initially negative (especially for **1a**·2$HClO_4$, **1a**·2*p*-TsOH, **1b**·2*p*-TsOH) and subsequently became positive. The small negative component in the response could be due to the coherent artifact.[35] The positive part decayed biexponentially. Similar behavior was observed for some of the corrole and cyclo[4]naphthobipyrrole derivatives studied earlier by us.[36,37] The data were fitted with a biexponential function (Table 4).[36,37] The slower component of the fits (1–2 ns, except for **1a** and **1b**) were almost comparable to

Table 3. Nonlinear absorption coefficients obtained from *Z*-scan measurements at 800 nm (estimated errors: ±15%).

Sample	I_{00} [$GW\,cm^{-2}$]	*c* [mM]	β [$cm\,W^{-1}$]×10^{-12}	n_2 [$cm^2\,W^{-1}$]×10^{-17}	σ_2 [GM]	Im$\lvert X^{(3)}\rvert$ [$m^2\,V^{-2}$]×10^{-23}	Re$\lvert X^{(3)}\rvert$ [$m^2\,V^{-2}$]×10^{-23}	$\lvert X^{(3)}\rvert$ [$m^2\,V^{-2}$]×10^{-23}	$\lvert X^{(3)}\rvert$ [e.s.u]×10^{-15}
1a	97	0.33	4.00	39.3	498	2.80	43.2	43.3	31.0
1a·2HCl	131	0.27	2.00	6.12	302	1.40	6.73	6.88	4.92
1a·2$HClO_4$	131	0.14	2.40	2.50	694	1.68	2.75	3.22	2.31
1a·H_2SO_4	131	0.24	2.00	6.60	339	1.40	7.26	7.4	5.30
1a·2*p*-TsOH	131	0.29	1.70	3.75	238	1.19	4.12	4.29	3.07
1b	107	0.34	3.70	63.6	447	2.59	70.0	70.0	50.1
1b·2HCl	123	0.30	2.00	10.4	274	1.40	11.4	11.5	8.26
1b·2$HClO_4$	128	0.07	2.00	2.12	1090	1.40	2.40	2.77	1.99
1b·H_2SO_4	136	0.23	1.65	1.87	295	1.15	2.05	2.36	1.69
1b·2*p*-TsOH	118	0.25	1.70	11.4	272	1.19	12.5	12.6	9.03

© 2014 Wiley-VCH Verlag GmbH & Co. KGaA, Weinheim

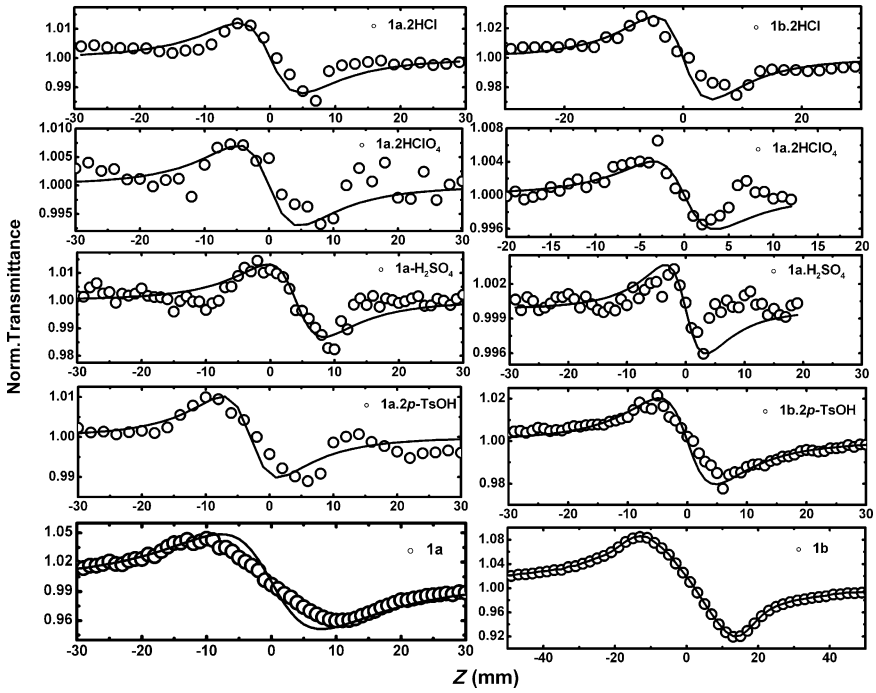

Figure 8. Closed-aperture *Z*-scan data at 800 nm. Open circles: experimental data; solid lines: theoretical fits.

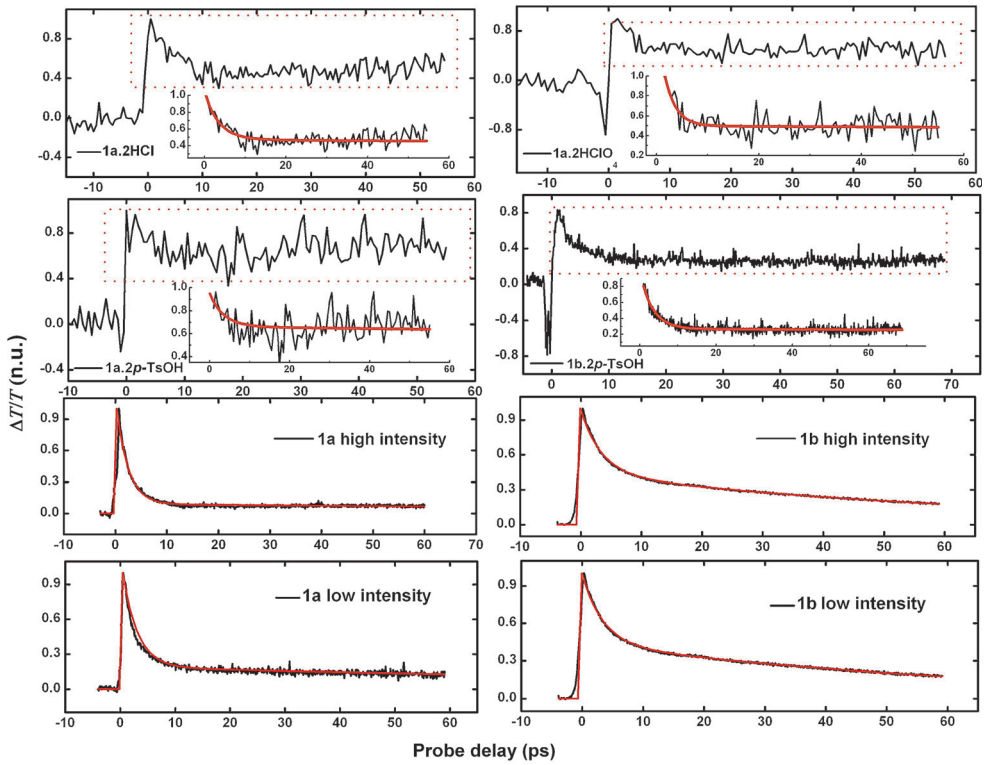

Figure 9. Degenerate pump–probe measurements at 800 nm. The pump and probe intensities were about 175 GW cm^{-2} and about 186 MW cm^{-2}, respectively. Black lines: experimental data; red lines: exponential fits. Degenerate pump–probe measurements of the free-base solutions of 0.3 mM concentration at 800 nm. The pump and probe intensities were about 100 GW cm^{-2} and about 186 MW cm^{-2}, respectively. Black lines: experimental data; red lines: exponential fits.

the radiative lifetimes (typically a few nanoseconds). In the case of **1a** and **1b** the slower decay components were about 184 and about 65 ps, respectively. Similar slower decay times were observed even for stronger pumping (at higher peak intensities, the decay components were ca. 150 and ca. 68 ps). These decay times probably have strong nonradiative components. The faster component (2–4 ps) can be attributed to the relaxation of population from high-lying singlet states including internal conversion (IC) from S_2 to S_1 states and intramolecular vibrational relaxation within S_2 sates. The two-photon excitation enables the population to reach S_2 states, and the slow decay includes the relaxation of population from the excited singlet state S_1 to S_0. The free-base sapphyrins **1a** and **1b** have longer radiative lifetimes (1.5–1.6 ns) compared to their *meso*-tetraaryl analogue **9** (1.3 ns), and this may be attributable to the greater structural flexibility in the latter due to free rotation of the *meso*-aryl substituents.[12] Expectedly, the lack of tautomerization due to absence of internal proton-transfer processes in the sapphyrin salts led to an increase in their radiative lifetimes (Table 4). Except for **1a**·H_2SO_4, all sapphyrins, including the free bases, showed single-exponential decay with lifetimes ranging from 1.50 to 2.18 ns, whereas the sulfate salt of **1a** exhibited double-exponential decay with lifetimes of 1.90 and 3.60 ns.

Nondegenerate pump–probe measurements

Nondegenerate pump–probe measurements were performed by using the same experimental setup that was used for degenerate pump–probe measurements. However, a 2-mm β-barium borate crystal was placed in the probe-beam path (no focusing of the probe beam was performed) and 400 nm photons were generated. A schematic of the nondegenerate pump–probe experiments is provided in

© 2014 Wiley-VCH Verlag GmbH & Co. KGaA, Weinheim

Table 4. Lifetimes of naphthosapphyrins. τ_1, τ_2 are the fitted parameters from the pump–probe data. Radiative lifetimes τ_r were obtained from time-correlated single-photon counting measurements.

Compound	Nondegenerate pump–probe data		Degenerate pump–probe data		Radiative lifetimes
	τ_1 [ps]	τ_2 [ns]	τ_1 [ps]	τ_2 [ns]	τ_r [ns]
1a	–	–	2.2 (91%), 2.7[a] (83%)	0.184 (9%), 0.150[a] (16%)	1.60
1a·2HCl	9 (24%)	1.8 (76%)	3.5 (55%)	1.5 (44%)	1.90
1a·2$HClO_4$	5 (18%)	1.8 (82%)	2.1 (68%)	2.0 (32%)	2.18
1a·H_2SO_4	9 (21%)	1.9 (79%)	–	–	1.90 (47.7%), 3.60 (52.3%)
1a·2*p*-TsOH	2 (13%)	2.2 (86%)	3.5 (31%)	1.5 (69%)	2.17
1b	–	–	3.4 (55%), 4.0[a] (55%)	0.065 (44%), 0.068[a] (44%)	1.50
1b·2HCl	3.8 (48%)	1.4 (52%)	–	–	1.59
1b·2$HClO_4$	2 (34%)	0.04 (65%)	–	–	2.00
1b·H_2SO_4	2 (20%)	1.0 (80%)	–	–	1.78
1b·2*p*-TsOH	4 (30%)	2.0 (70%)	3.2 (79%)	1.55 (21%)	1.90

[a] Data recorded with higher peak intensity of the pump ($\approx$175 GW cm^{-2}). Other degenerate pump–probe data were recorded at about 100 GW cm^{-2}. For nondegenerate pump–probe data the peak intensity of the pump was about 400 GW cm^{-2}.

the Supporting Information. Figure 10 shows the nondegenerate pump–probe data of **1a**·2HCl, **1a**·2$HClO_4$, **1a**·H_2SO_4, **1a**·2*p*-TsOH, **1b**·2HCl, **1b**·2$HClO_4$, **1b**·H_2SO_4, and **1b**·2*p*-TsOH. The data (Table 4) show a positive rise in differential transmission with biexponential decay, which again could be due to the relaxation of population in the higher excited singlet states (S_2) and IC from S_2 to S_1. The faster lifetimes were 2–9 ps and the slower decay times were 1–2.2 ns, except for **1b**·2$HClO_4$ ($\approx$40 ps), and the longer decay time matches well with the radiative lifetimes recorded independently. Since these compounds emit at about 730 nm (from the emission spectra), the second decay component could include contributions from both radiative and nonradiative processes. The dynamics of naphthosapphyrins are explained in detail by the schematic in Figure 11. The lower-energy excitations at 800 nm (degenerate case) were not sufficient to excite the molecules to S_2 states, except for the free-base molecules. Due to the nonlinearity of the free-base molecules, the lower-energy excitations permitted access to two-photon resonant states. The decays at this energy are biexponential and include intramolecular vibrational relaxation and IC followed by radiative or nonradiative decay. However, stronger pumping allowed the population to be excited to S_2 states.

In the nondegenerate pump–probe experiments, since pumping was performed at 400 nm, the excitation directly pumped the population into S_2 states and the double-exponential decays τ_1 and τ_2 (see Figure 11) followed. The data obtained from both degenerate and nondegenerate studies matched very well within the experimental errors. For example, the values of τ_2 obtained for **1a**·2$HClO_4$ were 1.8 and 2.0 ns in the nondegenerate and degenerate case, respectively. This value again matches with the radiative lifetime of 2.18 ns obtained from time-correlated single photon counting studies. The nonradiative de-excitation in case of free-base sapphyrins **1a** and **1b** can be attributed to the NH tautomerization processes and, intriguingly, **1b**·2$HClO_4$ also follows a similar path, unlike the other sapphyrin salts, which undergo de-excitation from the S_1 state via radiative paths, which is beyond our understanding at this stage.

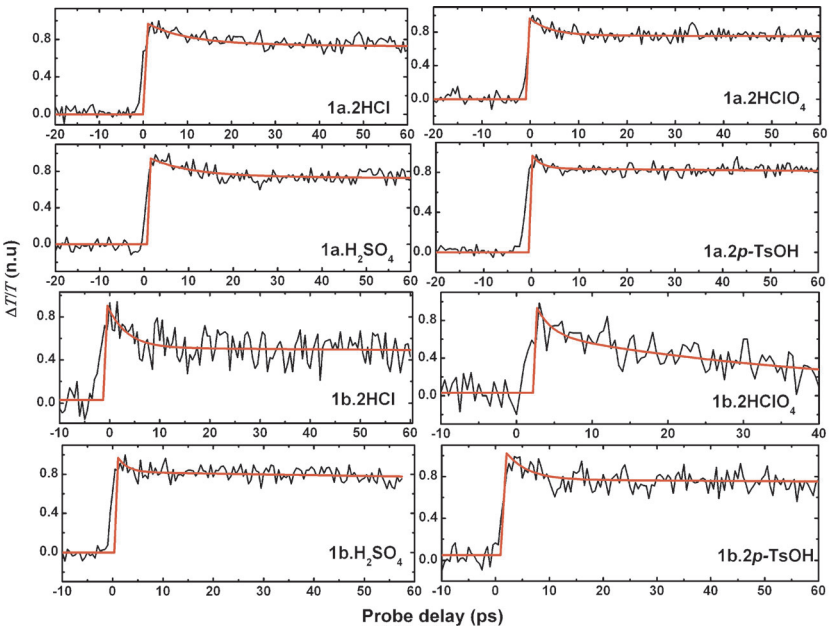

Figure 10. Nondegenerate pump–probe measurements (pump at 400 nm and probe at 800 nm). The pump and probe intensities were 440 GW cm^{-2} and 186 MW cm^{-2}, respectively. Black lines: experimental data; red lines: exponential fits.

Conclusion

We have synthesized and characterized in detail two new naphthosapphyrins and various salts thereof. Although bipyrrole fusion at β,β positions led to an increase in the size of the sapphyrin core, it is not sufficient to cause the inversion of the opposite unsubstituted pyrrole unit.

© 2014 Wiley-VCH Verlag GmbH & Co. KGaA, Weinheim

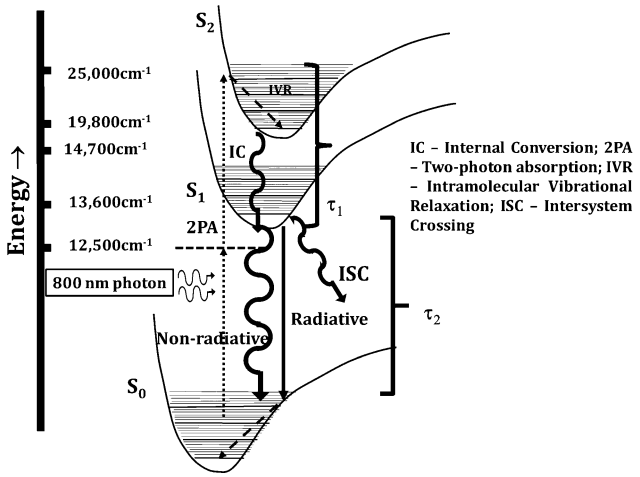

Figure 11. Energy-level diagram describing the various transitions involved once the population is excited into S_2 states through 2PA.

Further, an unprecedented aqua-bridged free-base sapphyrin dimer showing strong π–π stacking interaction in the solid state was isolated. Due to the higher nonlinearity of the free bases, 2PA was observed even at lower peak intensities, whereas the sapphyrin salts needed higher peak intensities. Excited-state dynamics studies by degenerate and nondegenerate pump–probe techniques revealed decay times of high-lying excited states in the pico- and nanosecond regimes.

Experimental Section

General procedure for naphthosapphyrins (1 a)

β-Diisopropylnaphthobipyrrole dialdehyde[24] (**2**; 170 mg, 0.49 mmol) was placed in a 500 mL round-bottom flask containing absolute ethanol (360 mL) and the mixture heated to reflux until no undissolved material remained. After cooling to room temperature, tripyrromethane dicarboxylic acid derivative **3 a** (210 mg, 0.49 mmol) was added, followed by the addition of *p*-TsOH·H_2O (378 mg, 1.96 mmol). The reaction mixture was protected from light and stirred for 24 h at room temperature with continuous oxygen bubbling. After completion of the reaction, the solvent was evaporated under reduced pressure, and the residual dark solid was dissolved in $CHCl_3$ and washed thoroughly with water. The organic layer was evaporated and the resulting residue was purified on a silica-gel column ($CHCl_3$ with increasing methanol content up to 10 vol% as eluent). The green fraction thus obtained was collected and washed with 1 M aqueous NaOH solution to obtain sapphyrin **1 a** in free-base form. Repeated column chromatography was necessary to obtain the pure product. Yield: 57 mg, 18%. Diprotonated salts were obtained by washing a $CHCl_3$ solution of the free base with aqueous solutions of various acids.

Data for 1 a: ^{1}H NMR (400 MHz, $CDCl_3$, ppm): $\delta = -0.53$ (brs, 3H, NH), 2.08 (brs, 6H, CH_3 Et), 2.65 (brd, 12H, CH_3 *i*Pr), 3.96 (s, 12H, CH_3 Me), 4.52 (brd, 4H, CH_2 Et), 5.74 (m, 2H, CH *i*Pr), 7.94 (m, 2H, CH naph), 9.41 (m, 2H, CH naph), 10.92 (s, 2H, CH *meso*), 11.26 (s, 2H, CH *meso*); HRMS (ESI): *m/z* calcd for $C_{44}H_{48}N_5$ $[M+H]^+$: 646.3910; found: 646.3909; UV/Vis ($CHCl_3$): λ_{max} (ε): 335 (21343), 468 (130921), 488 (156565), 624 (4724), 671 (14845), 689 (10942), 730 (17024), 765 nm (3065).

Data for 1 a·2HCl: ^{1}H NMR (400 MHz, $CDCl_3$, ppm): $\delta = -4.37$ (s, 2H, NH), −3.64 (s, 1H, NH), −3.17 (s, 2H, NH), 2.30 (t, $J = 7.2$ Hz, 6H, CH_3 Et,), 2.68 (d, $J = 6.8$ Hz, 12H, CH_3 *i*Pr), 4.14 (s, 12H, CH_3 Me), 4.65 (m, 4H, CH_2 Et), 5.79 (m, 2H, CH *i*Pr), 8.01 (m, 2H, CH naph), 9.50 (m, 2H, CH naph), 11.54 (s, 2H, CH *meso*), 11.85 (s, 2H, CH *meso*).

Data for 1 a·2HClO$_4$: ^{1}H NMR (400 MHz, $CDCl_3$, ppm): $\delta = -6.41$ (s, 2H, NH), −5.51 (s, 1H, NH), −5.14 (s, 2H, NH), 2.29 (t, $J = 7.6$ Hz, 6H, CH_3 Et), 2.66 (d, $J = 7.2$ Hz, 12H, CH_3 *i*Pr), 4.18 (s, 12H, CH_3 Me), 4.67 (q, $J = 7.2$ Hz, 4H, CH_2 Et), 5.75 (m, 2H, CH *i*Pr), 8.08 (m, 2H, CH naph), 9.63 (m, 2H, CH naph), 11.63 (s, 2H, CH *meso*), 11.95 (s, 2H, CH *meso*).

Data for 1 a·2*p*-TsOH: ^{1}H NMR (400 MHz, $CDCl_3$, ppm): $\delta = -4.88$ (s, 2H, NH), −4.26 (s, 1H, NH), −4.05 (s, 2H, NH), 2.36 (m, 6H, CH_3 Et), 2.74 (d, $J = 7.2$ Hz, 12H, CH_3 *i*Pr), 4.10 (s, 12H, CH_3 Me), 4.61 (q, $J = 7.2$ Hz, 4H, CH_2 Et), 5.41 (s, 4H, Ph *p*-TsOH), 5.73 (m, 2H, CH *i*Pr), 8.03 (m, 2H, CH naph), 9.45 (m, 2H, CH naph), 11.37 (s, 2H, CH *meso*), 11.75 (s, 2H, CH *meso*).

Data for 1 a·H$_2$SO$_4$: ^{1}H NMR (400 MHz, $CDCl_3$, ppm): $\delta = -4.34$ (s, 2H, NH), −3.71(s, 1H, NH), −3.16 (s, 2H, NH), 2.27 (brs, 6H, CH_3 Et), 2.69 (brs, 12H, CH_3 *i*Pr), 4.15 (brs, 12H, CH_3 Me), 4.66 (brs, 4H, CH_2 Et), 5.79 (brs, 2H, CH *i*Pr), 8.03 (s, 2H, CH naph), 9.52 (s, 2H, CH naph), 11.54 (s, 2H, CH *meso*), 11.85 (brs, 2H, CH *meso*).

Data for 1 b: Yield 26%; ^{1}H NMR (400 MHz, $CDCl_3$, ppm): $\delta = -0.95$ (brs, 3H, NH), 2.68 (d, $J = 7.2$ Hz, 12H, CH_3 *i*Pr), 3.83 (s, 6H, CH_3 Me), 3.86 (s, 6H, CH_3 Me), 5.65 (m, 2H, CH *i*Pr), 7.96 (m, 2H, CH naph), 9.38 (m, 2H, CH naph), 9.55 (s, 2H, CH Py), 10.20 (s, 2H, CH *meso*), 10.74 (s, 2H, CH *meso*); HRMS (ESI): *m/z* calcd for $C_{40}H_{40}N_5$ $[M+H]^+$: 590.3284; found 590.3286; UV/Vis ($CHCl_3$): λ_{max} (ε): 335 (20735), 465 (105402), 486 (109862), 615 (5884), 670 (13220), 690 (11324), 733 (14325), 771 nm (4526).

Data for 1 b·2 HCl: ^{1}H NMR (400 MHz, $CDCl_3$, ppm): $\delta = -4.81$ (brs, 2H, NH), −3.56 (brs, 1H, NH), −3.54 (brs, 2H, NH), 2.71 (d, $J = 7.2$ Hz, 12H, CH_3 *i*Pr), 4.19 (s, 12H, CH_3 Me), 5.81 (m, 2H, CH *i*Pr), 8.02 (m, 2H, CH naph), 9.52 (m, 2H, CH naph), 10.36 (s, 2H, CH Py), 11.65 (s, 2H, CH *meso*), 11.96 (s, 2H, CH *meso*).

Data for 1 b·2 TFA: ^{1}H NMR (400 MHz, $CDCl_3$, ppm): $\delta = -5.13$ (brs, 2H, NH), −3.99 (brs, 1H, NH), −3.91 (brs, 2H, NH), 2.67 (brs, 12H, CH_3 *i*Pr), 4.20 (s, 12H, CH_3 Me), 5.79 (m, 2H, CH *i*Pr), 8.07 (m, 2H, CH naph), 9.56 (m, 2H, CH naph), 10.43 (s, 2H, CH Py), 11.65 (s, 2H, CH *meso*), 11.99 (s, 2H, CH *meso*).

Data for 1 b·2*p*-TsOH: ^{1}H NMR (400 MHz, $CDCl_3$, ppm): $\delta = -5.26$ (brs, 2H, NH), −4.43 (brs, 2H, NH), −4.19 (brs, 1H, NH), 2.76 (brs, 12H, CH_3 *i*Pr), 4.13 (s, 12H, CH_3 Me), 5.33 (s, 4H, Ph *p*-TsOH), 5.77 (m, 2H, CH *i*Pr), 8.05 (m, 2H, CH naph), 9.48 (m, 2H, CH naph), 10.31 (s, 2H, CH Py), 11.48 (s, 2H, CH *meso*), 11.83 (s, 2H, CH *meso*).

1 b·2 HClO$_4$ and 1 b·H$_2$SO$_4$: Spectra could not be recorded due to very poor solubility.

Acknowledgements

This work is supported by Department of Science and Technology (DST), India (SR/S1/IC-56/2012 to P.K.P., SR/S1.JCB-02/2009 to Professor A. Samanta, School of Chemistry, University of Hyderabad) and Defence Research & Development Organization (DRDO), India. T.S. and A.P. thank Council of Scientific and Industrial Research (CSIR), India, for senior research fellowships.

Keywords: expanded porphyrins · excited-state dynamics · porphyrinoids · nonlinear optics · sapphyrins

© 2014 Wiley-VCH Verlag GmbH & Co. KGaA, Weinheim

[1] a) M. Shionoya, H. Furuta, V. Lynch, A. Harriman, J. L. Sessler, *J. Am. Chem. Soc.* **1992**, *114*, 5714; b) J. L. Sessler, J. M. Davis, *Acc. Chem. Res.* **2001**, *34*, 989; c) J. L. Sessler, S. Camiolo, P. A. Gale, *Coord. Chem. Rev.* **2003**, *240*, 17.

[2] a) B. G. Maiya, M. Cyr, A. Harriman, J. L. Sessler, *J. Phys. Chem.* **1990**, *94*, 3597; b) V. Král, J. Davis, A. Andrievsky, J. Kralova, A. Synytsya, P. Pouckova, J. L. Sessler, *J. Med. Chem.* **2002**, *45*, 1073; c) Z. Wang, P. Lecane, P. Thiemann, A. Fan, C. Cortez, X. Ma, D. Tonev, D. Miles, A. Lin, G. Hemmi, L. Naumovski, R. A. Miller, D. Magda, D.-G. Cho, J. L. Sessler, B. L. Pike, S. M. Yeligar, M. W. Karaman, J. G. Hacia, *Mol. Cancer* **2007**, *6*, 9; d) J. D. Hooker, V. H. Nguyen, V. M. Taylor, D. L. Cedeño, T. D. Lash, M. A. Jones, S. M. Robledo, I. D. Vélez, *Photochem. Photobiol.* **2012**, *88*, 194.

[3] a) S. K. Pushpan, T. K. Chandrashekar, *Pure Appl. Chem.* **2002**, *74*, 2045; b) R. Misra, T. K. Chandrashekar, *Acc. Chem. Res.* **2008**, *41*, 265.

[4] a) J. L. Sessler, D.-G. Cho, M. Stępień, V. Lynch, J. Waluk, Z. S. Yoon, D. Kim, *J. Am. Chem. Soc.* **2006**, *128*, 12640; b) I. Gupta, A. Srinivasan, T. Morimoto, M. Toganoh, H. Furuta, *Angew. Chem.* **2008**, *120*, 4639; *Angew. Chem. Int. Ed.* **2008**, *47*, 4563; c) S. K. Pushpan, A. Srinivasan, V. G. Anand, S. Venkatraman, T. K. Chandrashekar, B. S. Joshi, R. Roy, H. Furuta, *J. Am. Chem. Soc.* **2001**, *123*, 5138.

[5] P. J. Chmielewski, L. Latos-Grażyński, K. Rachlewicz, *Chem. Eur. J.* **1995**, *1*, 68.

[6] A. Srinivasan, V. G. Anand, S. J. Narayanan, S. K. Pushpan, M. R. Kumar, T. K. Chandrashekar, K.-I. Sugiura, Y. Sakata, *J. Org. Chem.* **1999**, *64*, 8693.

[7] a) S. J. Narayanan, B. Sridevi, T. K. Chandrashekar, A. Vij, R. Roy, *J. Am. Chem. Soc.* **1999**, *121*, 9053; b) S. J. Narayanan, B. Sridevi, T. K. Chandrashekar, A. Vij, R. Roy, *Angew. Chem.* **1998**, *110*, 3582; *Angew. Chem. Int. Ed.* **1998**, *37*, 3394.

[8] K. Shin, C. Lim, C. Choi, Y. Kim, C.-H. Lee, *Chem. Lett.* **1999**, *28*, 1331.

[9] T. Okujima, T. Kikkawa, S. Kawakami, Y. Shimizu, H. Yamada, N. Ono, H. Uno, *Tetrahedron* **2010**, *66*, 7213.

[10] a) P. K. Panda, Y.-J. Kang, C.-H. Lee, *Angew. Chem.* **2005**, *117*, 4121; *Angew. Chem. Int. Ed.* **2005**, *44*, 4053; b) N. Ono, K. Kuroki, E. Watanabe, N. Ochi, H. Uno, *Heterocycles* **2004**, *62*, 365.

[11] a) K. Rachlewicz, N. Spurtta, L. Latos-Grażyński, P. J. Chmielewski, L. Szterenberg, *J. Chem. Soc. Perkin Trans. 2* **1998**, 959; b) C. Brückner, E. D. Sternberg, R. W. Boyle, D. Dolphin, *Chem. Commun.* **1997**, 1689.

[12] S.-Y. Kee, J. M. Lim, S.-J. Kim, J. Yoo, J.-S. Park, T. Sarma, V. M. Lynch, P. K. Panda, J. L. Sessler, D. Kim, C.-H. Lee, *Chem. Commun.* **2011**, *47*, 6813.

[13] M. Sheik-Bahae, A. A. Said, T. H. Wei, D. J. Hagan, E. W. Van Stryland, *IEEE J. Quantum Electron.* **1990**, *26*, 760.

[14] V. V. Roznyatovskiy, C.-H. Lee, J. L. Sessler, *Chem. Soc. Rev.* **2013**, *42*, 1921.

[15] S. Saito, A. Osuka, *Angew. Chem.* **2011**, *123*, 4432; *Angew. Chem. Int. Ed* **2011**, *50*, 4342.

[16] K. V. Saravanan, K. C. James Raju, M. G. Krishna, S. P. Tewari, S. Venugopal Rao, *Appl. Phys. Lett.* **2010**, *96*, 232905.

[17] G. K. Podagatlapalli, S. Hamad, S. Sreedhar, S. P. Tewari, S. Venugopal Rao, *Chem. Phys. Lett.* **2012**, *530*, 93.

[18] a) R. S. S. Kumar, S. Venugopal Rao, L. Giribabu, D. Narayana Rao, *Chem. Phys. Lett.* **2007**, *447*, 274; b) S. Venugopal Rao, *J. Mod. Opt.* **2011**, *58*, 1024.

[19] a) D. Swain, P. T. Anusha, T. S. Prashant, S. P. Tewari, T. Sarma, P. K. Panda, S. Venugopal Rao, *Appl. Phys. Lett.* **2012**, *100*, 141109; b) S. Venugopal Rao, T. S. Prashant, D. Swain, T. Sarma, P. K. Panda, S. P. Tewari, *Chem. Phys. Lett.* **2011**, *514*, 98.

[20] D. Swain, R. Singh, V. K. Singh, N. V. Krishna, L. Giribabu, S. Venugopal Rao, *J. Mater. Chem. C* **2014**, *2*, 1711.

[21] P. T. Anusha, P. S. Reeta, L. Giribabu, S. P. Tewari, S. Venugopal Rao, *Mater. Lett.* **2010**, *64*, 1915.

[22] B. S. Singh, H. R. Lobo, G. K. Podagatlapalli, S. Venugopal Rao, G. S. Shankarling, *Opt. Mater.* **2013**, *35*, 962.

[23] D. Swain, V. K. Singh, N. V. Krishna, L. Giribabu, S. Venugopal Rao, *J. Porphyrins Phthalocyanines* **2014**, *18*, 305.

[24] a) T. Sarma, P. K. Panda, P. T. Anusha, S. V. Rao, *Org. Lett.* **2011**, *13*, 188; b) V. Roznyatovskiy, V. Lynch, J. L. Sessler, *Org. Lett.* **2010**, *12*, 4424.

[25] J. L. Sessler, M. R. Johnson, V. Lynch, *J. Org. Chem.* **1987**, *52*, 4394.

[26] V. J. Bauer, D. L. J. Clive, D. Dolphin, J. B. Paine, F. L. Harris, M. M. King, J. Loder, S. W. C. Wang, R. B. Woodward, *J. Am. Chem. Soc.* **1983**, *105*, 6429.

[27] CCDC 1006523 (**1a**·2HCl), 1006524 (**1a**·CH_3COOH) and 1006525 (**1b**) contain the supplementary crystallographic data for this paper. These data can be obtained free of charge from The Cambridge Crystallographic Data Centre via www.ccdc.cam.ac.uk/data_request/cif.

[28] J. L. Sessler, J. Lisowski, K. A. Boudreaux, V. Lynch, J. Barry, T. J. Kodadek, *J. Org. Chem.* **1995**, *60*, 5975.

[29] J. L. Sessler, M. J. Cyr, V. Lynch, E. McGhee, J. A. Ibers, *J. Am. Chem. Soc.* **1990**, *112*, 2810.

[30] While trying to crystallize **1a** in its free-base form, we isolated **1a** as its monoacetate salt. Although we did not use any source of acetate ion during crystallization, presumably it came from contaminated solvent used for crystallization under ordinary laboratory conditions.

[31] J. L. Sessler, A. Andrievsky, V. Lynch, *J. Am. Chem. Soc.* **1997**, *119*, 9385.

[32] J. L. Sessler, A. Andrievsky, P. A. Gale, V. Lynch, *Angew. Chem.* **1996**, *108*, 2954; *Angew. Chem. Int. Ed. Engl.* **1996**, *35*, 2782.

[33] O. Ohno, Y. Kaizu, H. Kobayashi, *J. Chem. Phys.* **1985**, *82*, 1779.

[34] Z. S. Yoon, D.-G. Cho, K. S. Kim, J. L. Sessler, D. Kim, *J. Am. Chem. Soc.* **2008**, *130*, 6930.

[35] M. V. Lebedev, O. V. Misochko, T. Dekorsy, N. Georgiev, *J. Exp. Theor. Phys.* **2005**, *100*, 272.

[36] P. T. Anusha, D. Swain, S. Hamad, L. Giribabu, T. S. Prashant, S. P. Tewari, S. Venugopal Rao, *J. Phys. Chem. C* **2012**, *116*, 17828.

[37] D. Swain, P. T. Anusha, T. Sarma, P. K. Panda, S. Venugopal Rao, *Chem. Phys. Lett.* **2013**, *580*, 73.

Received: June 5, 2014
Published online on September 26, 2014

 © 2014 Wiley-VCH Verlag GmbH & Co. KGaA, Weinheim